Deformation characteristics of aluminium–copper composite preforms at different strain rates during cold forging

Article *in* International Journal of Materials and Product Technology · January 2017

DOI: 10.1504/IJMPT.2017.10000796

CITATION
1

READS
146

3 authors, including:

Rk Ranjan
Government Polytechnic, Lakhisarai
26 PUBLICATIONS **14** CITATIONS
SEE PROFILE

Surender Kumar
31 PUBLICATIONS **174** CITATIONS
SEE PROFILE

Deformation characteristics of aluminium-copper composite preforms at different strain rates during cold forging

Shrikant Jain* and R.K. Ranjan

Department of Mechanical Engineering,
GGITS, Jabalpur, India
Email: shrikant.ggits@gmail.com
Email: rkranjanbit@gmail.com
*Corresponding author

Surendra Kumar

Department of Mechanical Engineering,
GLA University,
Mathura (U.P.), India
Email: kr.surender@gmail.com

Abstract: The paper presents an investigation into the deformation characteristics of aluminium-copper composite preforms at different strain rates (based on ram velocity) during cold forging under lubricated end conditions. The preforms were prepared and forged at different ram velocities: 1.5, 50, 100 and 150 mm/min. The forgeability of all the composite preforms was noted when cracks were observed on the equatorial free surfaces at corresponding percent reduction in height. The yield criterion as proposed by Tabata and Masaki, composite friction law, an appropriate velocity field, a mathematical model considering 'upper bound' analysis was developed for relative average forging pressure on the platen during cold forging of the composite preform at different ram velocities. Theoretical results have been presented graphically showing the variation of the relative average forging pressure versus percent reduction in height of these composite preforms. Experimentally obtained forgeability of different composite preforms at different ram velocities have been plotted with respect to: 1) percent reduction in height; 2) forging stress; 3) compressive strength; 4) percent increase in bulge diameter; 5) linear hoop strain. Theoretical and experimentally obtained values of relative average forging pressure versus percent reduction in height of the preform were plotted for different composite-preforms and a good correlation was observed.

Keywords: composite preform; strain rate; yield criterion; interfacial friction law; forgeability; bulging.

Reference to this paper should be made as follows: Jain, S., Ranjan, R.K. and Kumar, S. (2017) 'Deformation characteristics of aluminium-copper composite preforms at different strain rates during cold forging', *Int. J. Materials and Product Technology*, Vol. 54, Nos. 1/2/3, pp.45–64.

Biographical notes: Shrikant Jain received his BE (honours) in Mech. Eng. (1970) from Government Engineering College Jabalpur (M.P.) India and ME in Aeronautical Eng. (1972–74) from Indian Institute of Science, Bangalore, India. He is a Senior Scientific Officer II in DR&D Lab. Hyderabad (A.P.) India (1974–76). In 1977, he established a production and processing unit at Jabalpur to cater the needs of defence establishments and the public. In 2004, he became a faculty and is currently a Professor in Mechanical Engineering Department at Gyan Ganga Institute of Technology and Sciences, Jabalpur (M.P.). He was awarded his PhD (2015) in the area of metallic composite forming from GLA University, Mathura (U.P.).

R.K. Ranjan received his MTech in Production from Institute of Technology, BHU, Varanasi, (U.P.) India, in 1997 and PhD in Metal Powder Forming from Birla Institute of Technology, Messara (Jharkhand) India in 2005. Currently, he is a Principal at Gyan Ganga College of Technology, Jabalpur India and Professor in the Department of Mechanical Engineering. His area of interest is metal powder forming. There are more than 50 research papers in his credit.

Surendra Kumar holds a BSc degree (1963), BE Mech. degree (1967), ME in Design and Production (University of Allahabad, 1969) and a PhD (Birla Institute of Technology, Ranchi University, 1975). He has 45 years professional experience. His academic achievement and awards include: Outstanding Research Paper Award, Institution of Engineers (I), 1984. He is a member of Tribological Society of India, Institution of Engineers (I), Indian Society of Value Engineering, Indian Institute of Production Engineers, European Association of Material Forming and Institute of Metals etc. He attended 20 international conferences, 30 national conferences, and 20 organised conferences. He has published in 108 journals, 62 international conferences, 88 national conferences and ten books.

1 Introduction

Composite metal powder preform forging has the advantages associated with conventional powder metallurgical processes along with additional strength provided by the elimination of porosity, had been discussed by Cull (1970). Jha and Kumar (1988) investigated the influence of powder particle sizes, compacting pressures, sintering temperatures, and forging parameters on relative density of the preform along with the deformation characteristics and fracture mechanisms during the cold forging of sintered iron powder preform under axis-symmetric conditions.

Chitkara and Bhutta (2001) in their investigation showed that in dynamic shape heading of triangular, hexagonal, and octagonal shaped heads from solid cylindrical aluminium specimens, the dynamic die loads were 20–40% higher than the static loading. Singh and Jha (2001) have analysed the dynamic effects during high speed forging of sintered preforms by energy method for axisymmetric and plain strain conditions. They have shown that die velocity has significant effect on deformation characteristics. Ranjan and Kumar (2004b) presented a generalised solution to determine die pressure for high speed forging of N-sided polygonal sintered powder disc. Ranjan and Kumar (2004a) had also used an upper bound approach to determine the die pressure in closed die forging of hexagonal preform and found the die pressure was minimum for certain dimensional ratios of the preform. Sumathi and Selvakumar (2012) have investigated the workability

of sintered copper-silicon carbide preforms during cold axial upsetting. They showed that strength property is very high at 5% of SiC with copper and the initiation of crack appeared at a low axial strain with higher value of SiC addition. Verma et al. (2013) have investigated the deformation characteristics during open-die forging of silicon carbide particulate reinforced aluminium metal matrix composites (Si-Cp AMC) at cold conditions. Authors have not yet come across the investigations in which the effect of strain rate (based on ram velocity) on the composite preform has been taken into consideration, as the strain rate is one of the most important parameter in forging process.

The present paper reports on an investigation into various technical aspects of the cold forging of aluminium-copper composite cylindrical preforms at different strain rates. A mathematical model has been developed showing the relative average forging pressure on the platen during cold forging at different ram velocities. The theoretical results have been presented graphically. The effect of ram velocities on deformation behaviour has been observed and discussed.

2 Basic equations

2.1 Yield criterion during plastic deformation of preform

Basic assumptions:

- The material is isotropic rigid plastic but compressible with volume inconsistency.
- The density distribution is non-uniform throughout the deforming process.
- Yielding is sensitive to hydrostatic stress.
- Deformation is inhomogeneous and barrelling is considered.
- Coefficient of friction is constant, and both sliding and sticking friction are considered. The friction due to adhesion (sticking friction) is a function of relative density ρ_r.
- Forging die-faces are flat and rigid.
- Pressure is normal to the contact-surfaces.
- Elastic deformation is neglected.

Tabata and Masaki (1978) proposed yield criterion;

$$\rho^k \sigma_0 = \sqrt{3J_2'} \pm 3\eta\sigma_m \tag{1}$$

where negative sign is for compressive load and $\eta \leq 0$, η and k were determined experimentally:

$$\eta = 0.54(1-\rho)^{1.2},\ k = 2, \text{ for } \sigma_m \leq 0 \tag{2}$$

For axisymmetric conditions the equation (1) becomes

$$\sigma_1 = \frac{\rho^k \sigma_0}{(1-2\eta)} + \frac{(1+\eta)}{(1-2\eta)}\sigma_2 \tag{3}$$

The moment yielding starts, the equation reduces to give flow stress

$$\lambda = \frac{\rho^k \sigma_0}{(1-2\eta)} \tag{4}$$

According to Tabata and Masaki (1978) the principal strain increments are:

$$d\varepsilon_i = d\lambda \left[\frac{3(\sigma_i - \sigma_m)}{\sqrt[2]{3J_2'}} \pm \eta \right] (\text{for } i = 1, 2, 3) \tag{5}$$

where $d\lambda = \frac{\sqrt{2}}{3}\sqrt{(d\varepsilon_1 - d\varepsilon_2)^2 + (d\varepsilon_2 - d\varepsilon_3)^2 + (d\varepsilon_3 - d\varepsilon_1)^2}$ is a positive constant, the volumetric strain increment $d\varepsilon_v$ is

$$\begin{aligned} d\varepsilon_v &= d\varepsilon_1 + d\varepsilon_2 + d\varepsilon_3 = \pm 3\eta d\lambda \\ &= \pm\mu\sqrt{2}\eta\left[(d\varepsilon_1 - d\varepsilon_2)^2 + (d\varepsilon_2 - d\varepsilon_3)^2 + (d\varepsilon_3 - d\varepsilon_1)^2\right]^{1/2} \end{aligned} \tag{6}$$

For axisymmetric compression the compatibility equation becomes

$$\varepsilon_r = \frac{(2\eta - 1)}{2(\eta + 1)} \ln \frac{h_2}{h_1} \tag{7}$$

2.2 Interfacial friction law

Frictional conditions between deforming tool and work piece in metal forming are of great importance and depend on various factors as discussed by Deryagin (1952). During plastic deformation mechanism of composite friction occurs and the shear stress equation becomes

$$\tau = \mu\left(p + \rho_0 \phi_0\right) \tag{8}$$

modified for cylindrical preform as proposed by Rooks (1974)

$$\tau = \mu\left[\overline{p} + \rho_0 \phi_0 \left(1 - \frac{r_m - r}{n r_0}\right)\right] \tag{9}$$

sticking radius $r_m = r - (\frac{h}{2\mu}) \ln \frac{1}{\sqrt{3}\mu}$ and constant $n >> 1$.

2.3 Forging of cylindrical preform at different strain rates

2.3.1 Basic experiments and deformation pattern

The cylindrical preforms were fabricated from aluminium-copper powders, mixed in different proportions on weight percentage basis: 100:00, 95:05, 90:10, and 70:30 on 400 kN UTM at a compaction pressure of 300 MPa using a closed cavity circular die-set of 20 mm diameter as shown in Figure 1, and sintered at 500°C in endothermic atmosphere. The preform density was obtained simply by measuring dimensions and weight and the relative density was then obtained.

Figure 1 Die set used to fabricate cylindrical preform (see online version for colours)

These preforms had relative density of 0.9 (approximately) and aspect ratio 1.0. The preforms were forged on the forging machine of 400 kN capacity at different ram velocities: 1.5, 50, 100, and 150 mm/min with lubricated end conditions. Figure 2 shows the cylindrical preform before and after the deformation. The upper platen moves down ward with velocity U_0 and lower platen remains stationary. Care was taken to place the axis of the cylindrical preform concentric with the axis of the die and platen. After each deformation dimensions measured were: deformed height, bulging loads, and diameters at load end, bulged portion and lower end. The percent height reduction, average contact diameter, percent increase in diameters at top, bulged portion and bottom, and compressed volume, changed relative density of the preforms were calculated.

Figure 2 Cylindrical preform before and after deformation

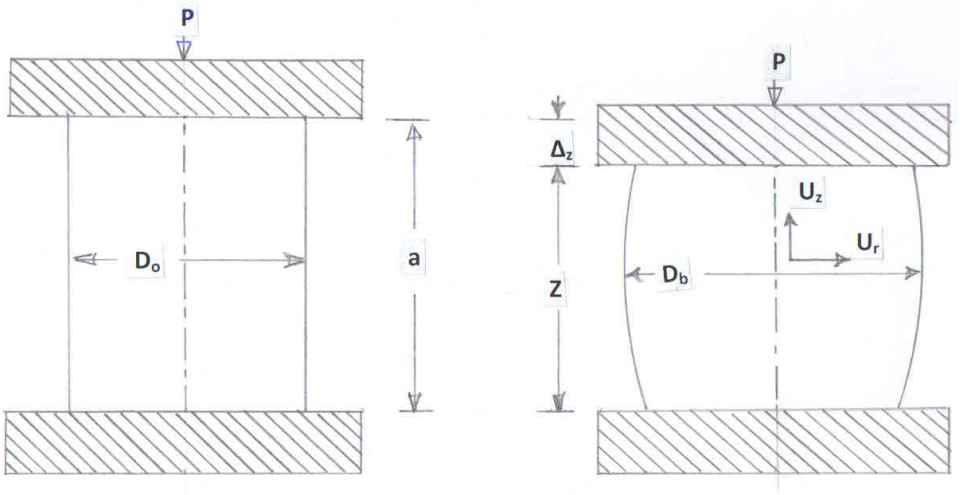

2.3.2 Velocity fields and strain rates

The velocity field was ascertained from the bulged profiles of the compressed preforms which match quite well with the velocity field chosen by Chitkara and Bhutta (2001). Considered kinematically admissible velocity fields are;

$$U_z = -\frac{2U_0 Z}{3a} - \frac{U_0 Z^2}{3a^2}\left\{2 - \frac{Z^2}{a^2}\right\} \tag{10}$$

$$U_\theta = 0 \tag{11}$$

$$U_r = K\left[\frac{U_0 r}{3a} + \frac{2U_0 Zr}{3a^2}\left\{1 - \frac{Z^2}{a^2}\right\}\right] \tag{12}$$

- *Strain rates*:

$$\dot{\varepsilon}_r = \frac{\partial U_r}{\partial r} = K\left[\frac{U_0}{3a} + \frac{2U_0 Z}{3a^2}\left\{1 - \frac{Z^2}{a^2}\right\}\right] \tag{13}$$

$$\dot{\varepsilon}_\theta = \frac{Ur}{r} + \frac{1}{r}\frac{\partial U_\theta}{\partial_\theta} = K\left[\frac{U_0}{3a} + \frac{2U_0 Z}{3a^2}\left\{1 - \frac{Z^2}{a^2}\right\}\right] = \dot{\varepsilon}_r \tag{14}$$

$$\dot{\varepsilon}_z = -2\left[\frac{U_0}{3a} + \frac{2U_0 Z}{3a^2}\left\{1 - \frac{Z^2}{a^2}\right\}\right] \tag{15}$$

K is determined using Tabata and Masaki (1978) compressibility equation:

$$(\dot{\varepsilon}_r + \dot{\varepsilon}_\theta + \dot{\varepsilon}_z) = \pm 2\eta\sqrt{(\dot{\varepsilon}_r - \dot{\varepsilon}_\theta)^2 + (\dot{\varepsilon}_\theta - \dot{\varepsilon}_z)^2 + (\dot{\varepsilon}_z - \dot{\varepsilon}_r)^2} \tag{16}$$

substituting strain rates value in equation (16) gives

$$K = \frac{(1-2\eta)}{(1+\eta)} \tag{17}$$

- *Internal power of deformation* (W_i):

$$\begin{aligned} W_i &= \frac{2}{\sqrt{3}}\sigma_0^* \int \sqrt{\frac{1}{2}\dot{\varepsilon}_{ij}\dot{\varepsilon}_{ij}}\, dv \quad \because dv = 2\pi r\, dr\, dz \\ W_i &= \frac{2\pi\sqrt{2}}{\sqrt{3}}\sigma_0^* \iint \sqrt{(\dot{\varepsilon}_r^2 + \dot{\varepsilon}_\theta^2 + \dot{\varepsilon}_z^2)}\, r\, dr\, dz \end{aligned} \tag{18}$$

substituting the values

$$\begin{aligned} W_i &= \frac{4\pi\sqrt{(K^2+2)}}{\sqrt{3}}\sigma_0^* \int_{r=0}^{r_0}\int_0^a \left[\frac{2U_0}{3a} + \frac{8U_0 Z}{3a^2}\left\{1 - \frac{4Z^2}{a^2}\right\}\right] r\, dr\, dz \\ &= \frac{\sqrt{(K^2+2)}}{\sqrt{3}}(\pi r_0^2)\sigma_0^* U_0 \end{aligned} \tag{19}$$

- *Frictional power losses* (W_f):

$$W_f = 2\times 2\pi \int_0^{r_{ex}} \tau |\Delta V| r\, dr \tag{20}$$

r_{ex} is new expanded radius of the preform. Using equation (9)

$$\tau = \mu\left[\bar{p} + \rho_0\phi_0\left(1 - \frac{r_m - r}{nr_0}\right)\right]$$

putting $\rho_0\phi_0 = x\bar{p}$ and after integration equation (20)

$$W_f = \frac{2\pi r_0^2 \bar{p} U_0}{9} K\mu\left(\frac{2r_0}{a}\right)\left(\frac{r_{ex}}{r_0}\right)^3\left[1 + x - \left(\frac{x}{n}\right)\left(\frac{r_m}{r_0}\right) + \frac{3}{4}\left(\frac{x}{n}\right)\left(\frac{r_{ex}}{r_0}\right)\right] \tag{21}$$

- *Energy dissipation due to inertia* (W_a):

$$W_a = \rho_p \int U_i \dot{U}_i\, dv \tag{22}$$

ρ_p – preform density.

$$W_a = 2\pi\rho_p \int_{z=0}^{a}\int_0^{r_0} \{U_r\dot{U}_r + U_\theta\dot{U}_\theta + U_z\dot{U}_z\} r\, dr\, dz$$

The acceleration components $\dot{U}_r, \dot{U}_\theta,$ and $\dot{U}_z$ are:

$$\dot{U}_r = \frac{\partial U_r}{\partial t} + U_r\frac{\partial U_r}{\partial r} + \frac{U_\theta}{r}\frac{\partial U_r}{\partial \theta} + U_z\frac{\partial U_r}{\partial z} - \frac{U_0^2}{r},$$

$$\dot{U}_\theta = \frac{\partial U_\theta}{\partial t} + U_r\frac{\partial U_\theta}{\partial r} + \frac{U_\theta}{r}\frac{\partial U_\theta}{\partial \theta} + U_z\frac{\partial U_\theta}{\partial z} + \frac{U_\theta U_r}{r},$$

$$\dot{U}_z = \frac{\partial U_z}{\partial t} + U_r\frac{\partial U_z}{\partial r} + \frac{U_\theta}{r}\frac{\partial U_z}{\partial \theta} + U_z\frac{\partial U_z}{\partial z}$$

substituting the values

$$\dot{U}_\theta = 0 \tag{23}$$

$$\begin{aligned}\dot{U}_r = {} & K\left[\frac{r}{3a} + \frac{2Zr}{3a^2}\left\{1 - \frac{Z^2}{a^2}\right\}\right]\left[\dot{U} - KU_0^2\left(\frac{1}{3a} + \frac{2Z}{3a^2}\left\{1 - \frac{Z^2}{a^2}\right\}\right)\right] \\ & + \frac{U_0^2}{r}\left[1 - \frac{2Kr}{3a^2}\left(1 - \frac{Z^2}{a^2}\right)\left\{\frac{2Z}{3a} + \frac{Z^2}{3a^2}\left(2 - \frac{Z^2}{a^2}\right)\right\}\right]\end{aligned} \tag{24}$$

$$\dot{U}_z = -\left[\dot{U} - U_0\left(\frac{2}{3a} + \frac{4z}{3a^2} - \frac{3z^2}{3a^2}\right)\right]\left[\frac{2Z}{3a} + \frac{Z^2}{3a^2}\left(2 - \frac{Z^2}{a^2}\right)\right] \tag{25}$$

substituting values in equation (22)

$$W_a = 2\pi r_0^2 U_0 \rho_p \left[\dot{U}_a \left\{ 0.0533K^2 \left(\frac{2r_0}{a} \right)^2 + 0.167 \right\} + U_0^2 \left\{ 0.011K^2 \left(\frac{2r_0}{a} \right)^2 + \frac{K}{4} + 0.056 \right\} \right] \tag{26}$$

- *External power J^* supplied by the press*:

$$J^* = W_i + W_f + W_a + W_t \tag{27}$$

W_t: predetermined body traction which is zero.

$$J^* = \int F_i U_0 \, ds = PU_0 = U_0 \int_0^{r_0} 2\pi r \bar{p} \, dr = \pi r_0^2 \bar{p} U_0 \tag{28}$$

$\bar{p}$ is average pressure.

substituting W_i, W_f, and W_a, the relative average forging pressure is:

$$\frac{\bar{p}}{\sigma_0^*} = \frac{\dfrac{\sqrt{(k^2+2)}}{\sqrt{3}} + \dfrac{2\rho_p}{\sigma_0^*} \left[\begin{array}{l} \dot{U}a \left\{ 0.0533K^2 \left(\dfrac{2r_0}{a} \right)^2 + 0.167 \right\} \\ + U_0^2 \left\{ 0.011K^2 \left(\dfrac{2r_0}{a} \right)^2 + 0.056 \right\} \end{array} \right]}{1 - \dfrac{2}{9} K\mu \left(\dfrac{2r_0}{a} \right) \left(\dfrac{r_{ex}}{r_0} \right)^3 \left[1 + x - \left(\dfrac{x}{n} \right) \left(\dfrac{r_m}{r_0} \right) + \dfrac{3}{4} \left(\dfrac{x}{n} \right) \left(\dfrac{r_{ex}}{r_0} \right) \right]} \tag{29}$$

The *dynamic effect* is defined as:

$$\zeta = \frac{\left| \dfrac{p_{av}}{\sigma_0^*} \right|_{\text{with dynamic effect}} - \left| \dfrac{p_{av}}{\sigma_0^*} \right|_{\text{without dynamic effect}}}{\left| \dfrac{p_{av}}{\sigma_0^*} \right|_{\text{with dynamic effect}}} \tag{30}$$

The variation of the theoretical relative average forging pressure on the surface of the preform versus percent reduction in height of the preform has been plotted using the equation (29) with appropriate multiplier. Figure 3(a) shows this variation at different values of ram velocities and it is observed that as the ram velocity increases, the relative average forging pressure also increases, for a given percent reduction in height for a particular initial density of the preform. For different values of coefficient of friction 'μ', and cohesive friction factor 'x', this variation of the relative average forging pressure versus percent reduction in height of the preform are shown in Figures 3(b) and 3(c). As these values are increased, the relative average forging pressure also increased, for a given percent reduction in height of the preform. If the value of constant 'n' is increased, the relative average forging pressure decreases for a considered percent reduction in height of specimen, as shown in Figure 3(d).

Figure 3 (a) Relative average forging pressure versus percent reduction in height (b) Relative average forging pressure versus percent reduction in height (c) Relative average forging pressure versus percent reduction in height (d) Relative average forging pressure versus percent reduction in height (see online version for colours)

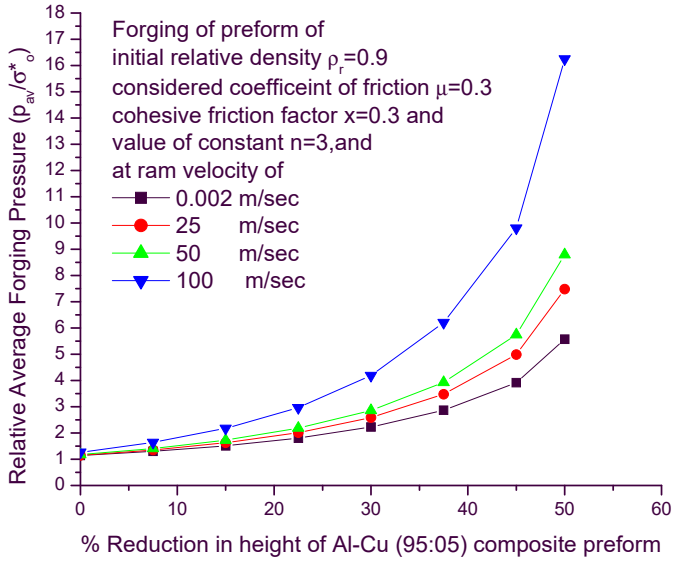

(a)

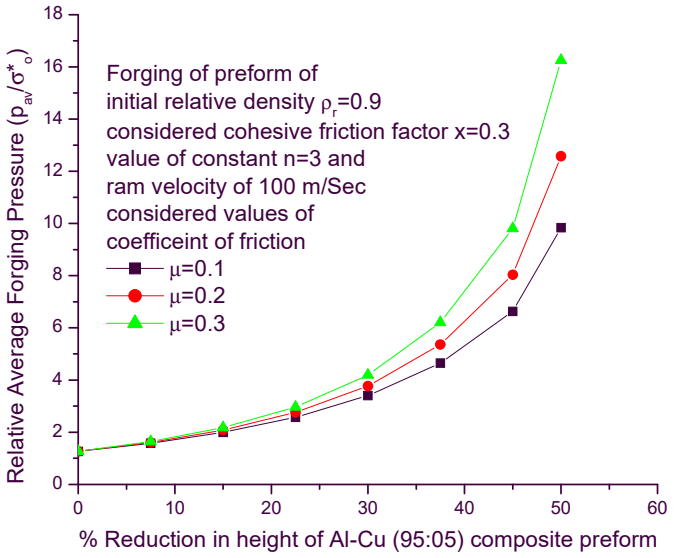

(b)

Figure 3 (a) Relative average forging pressure versus percent reduction in height (b) Relative average forging pressure versus percent reduction in height (c) Relative average forging pressure versus percent reduction in height (d) Relative average forging pressure versus percent reduction in height (continued) (see online version for colours)

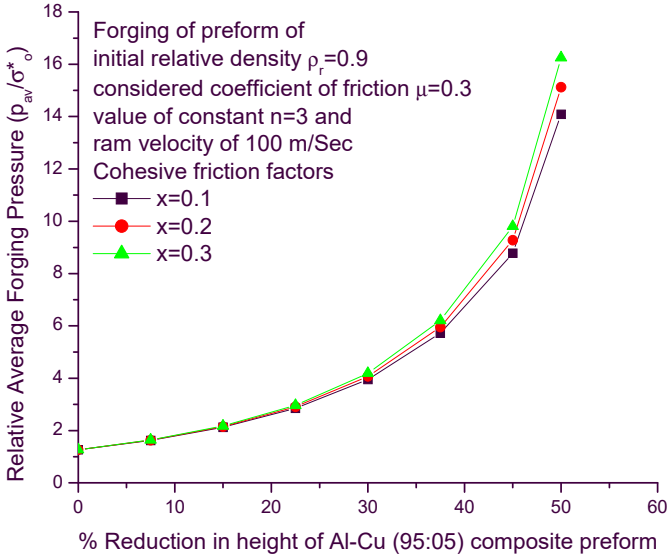

(c)

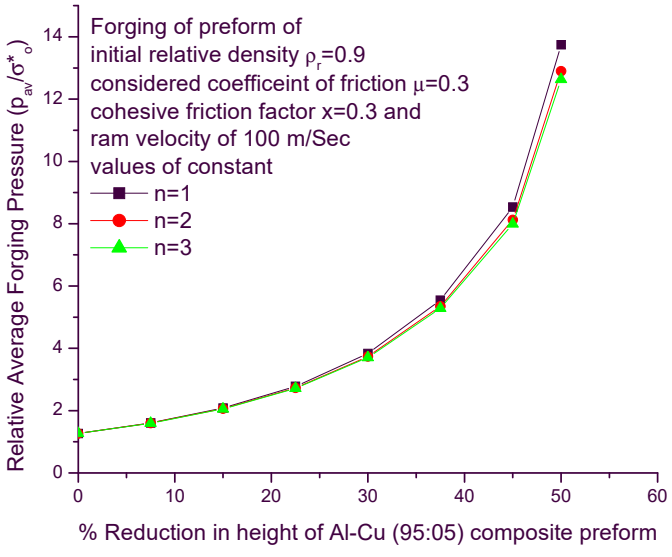

(d)

The variation of the theoretical relative average forging pressure versus ram velocity at 50% reduction in height for different relative densities of the specimens is shown in Figure 4. The dynamic effect variation versus ram velocity for different relative densities of the preforms is shown in Figure 5. As the relative density of the preform increases, the relative average forging pressure and the dynamic effect also increases for considered ram velocity.

Figure 4 Relative average forging pressure versus ram velocity (see online version for colours)

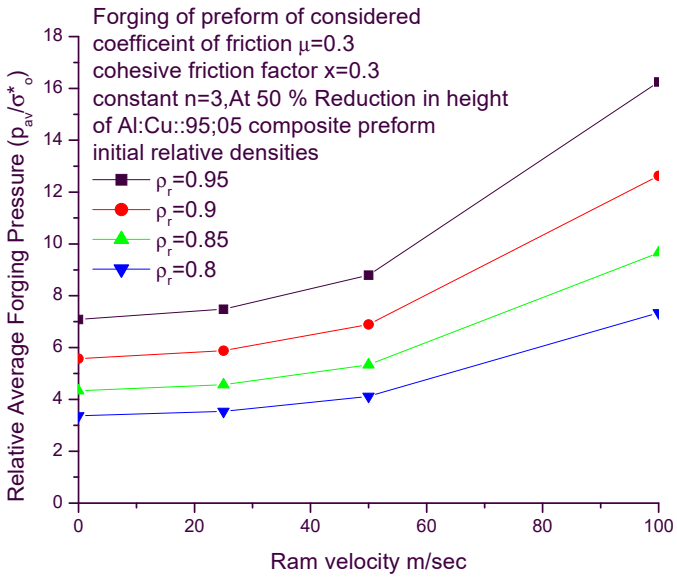

Figure 5 Dynamic effects versus ram velocity (see online version for colours)

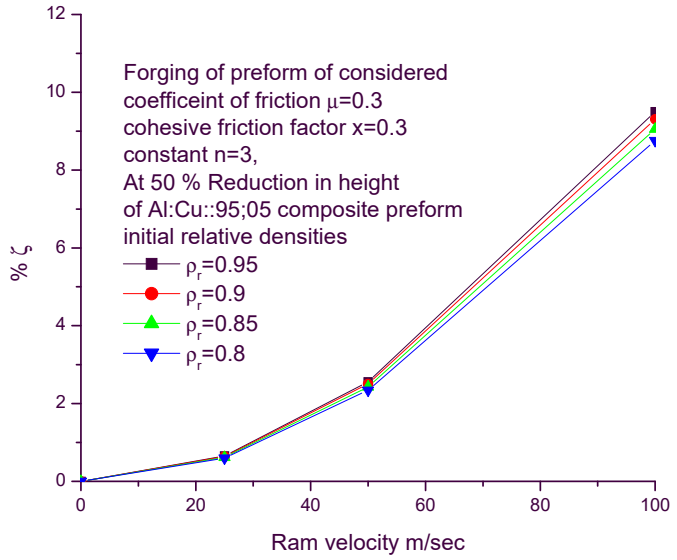

3 Experimental varification

The density and modulus of elasticity of composite solid metal were calculated as under:

- the density $\rho_{\text{AlCu}} = \left[\dfrac{100}{\left(\dfrac{\%\text{ of Al}}{\rho_{\text{Al}}} \right) + \left(\dfrac{\%\text{ of Cu}}{\rho_{\text{Cu}}} \right)} \right]$

- the modulus of elasticity $E_{\text{AlCu}} = \left[\dfrac{\left(\dfrac{\%\text{ of Al}}{\rho_{\text{Al}}} \right) E_{\text{Al}} + \left(\dfrac{\%\text{ of Cu}}{\rho_{\text{Cu}}} \right) E_{\text{Cu}}}{\left(\dfrac{\%\text{ of Al}}{\rho_{\text{Al}}} \right) + \left(\dfrac{\%\text{ of Cu}}{\rho_{\text{Cu}}} \right)} \right]$

The density of aluminium and copper metals were considered as 2.7 gm/cm^3 and 8.94 gm/cm^3 and modulus of elasticity as 70 GPa and 120 GPa respectively. The flow stress 'σ_0' for the composite was calculated at strain value of 0.15%. The composite-preforms of considered aluminium-copper compositions were prepared (had relative density of 0.9 approximately) and forged at different ram velocities: 1.5, 50, 100 and 150 mm/min, and these compressed composite preforms are shown in Figures 7(a), 7(b), 7(c) and 7(d) respectively. In this paper, only the experimental results of the forging done at ram velocity of 1.5 mm/min had been considered. The relative density of the compressed preform increases with the reduction in height due to forging. These results were superimposed on the theoretically results using equation (29) with appropriate multiplier and plotted for the variation of the relative average forging pressure versus percent reduction in height as shown in Figures 6(a), 6(b), 6(c) and 6(d) for considered coefficient of friction as 0.3, cohesive factor 'x' as 0.3 and constant n = 3 with different relative densities of preform as 0.9, 0.95 and 0.98.

Figure 6(a) is for aluminium preform, it is observed that as the forging pressure increases, the compressed preform density increases, which is evident from the experimental curve intersecting the theoretical curves. The deformation is gradual, resulting in smooth barrelling with appearance of crack on equatorial free surface at 52% height reduction. In Figure 7(a), the compressed aluminium preform shows smooth barrelling. Figure 6(b) is for Al:Cu (95:05) composite preform, only 5% copper had been added which has slightly affected the deformation behaviour and crack appeared at 40% height reduction of the preform as shown in Figure 7(a). Figure 6(c) is for Al:Cu (90:10) composite preform, with further increase in copper percentage up to 10, the deformation behaviour is further affected and crack appeared at 35% height reduction of the preform as shown in Figure 7(a). But in Figure 6(d) which is for Al:Cu (70:30) composite preform, copper percentage was increased up to a high level of 30%. This high copper percentage has drastically changed the deformation behaviour and high brittleness was observed and crack appeared at 18% height reduction of the preform as shown in Figure 7(a). By observing the compressed composite preforms [shown in Figures 7(b), 7(c) and 7(d)], forged at different ram velocities: 50, 100 and 150 mm/min, the effect of increased strain rates resulted in the appearance of creaks at deceasing order of percent height reduction of the preforms. This was due to the reduction of ductility with the increasing percentage of copper in the composite preforms and for copper up to 5% the

ductility was reasonably good, but as the percentage of copper increased resulted in the increased brittleness and the appearance of crack on the preform at early stage.

Figure 6 (a) Relative average forging pressure versus percent reduction in height
(b) Relative average forging pressure versus percent reduction in height
(c) Relative average forging pressure versus percent height reduction
(d) Relative average forging pressure versus percent height reduction
(see online version for colours)

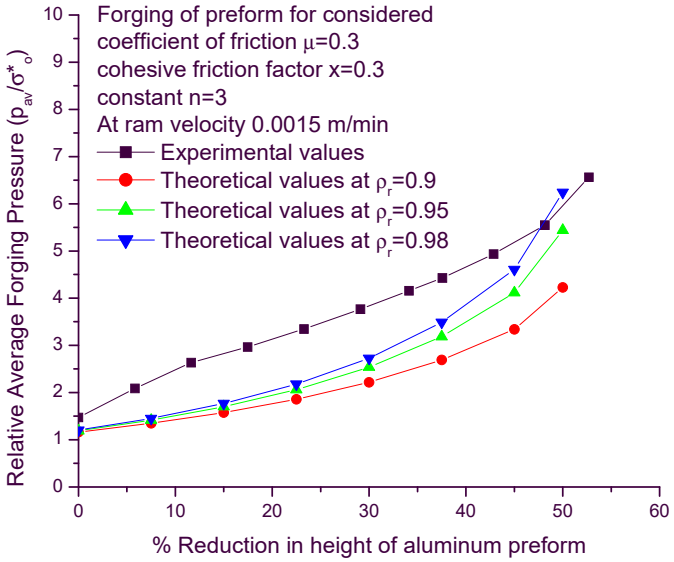

(a)

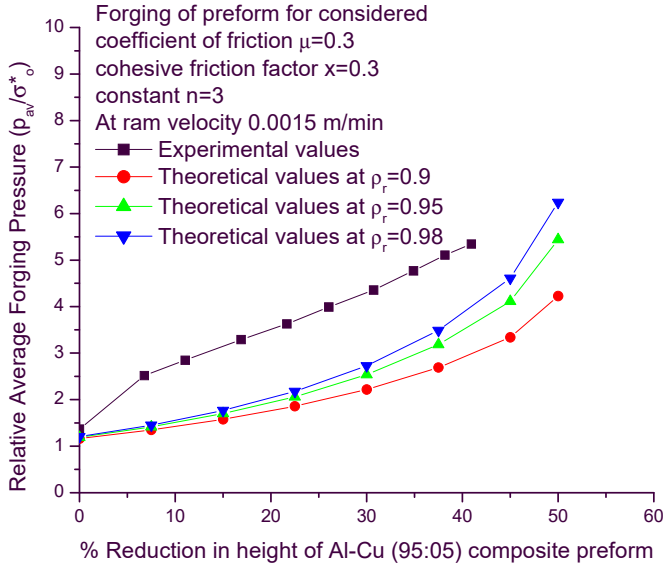

(b)

Figure 6 (a) Relative average forging pressure versus percent reduction in height (b) Relative average forging pressure versus percent reduction in height (c) Relative average forging pressure versus percent height reduction (d) Relative average forging pressure versus percent height reduction (continued) (see online version for colours)

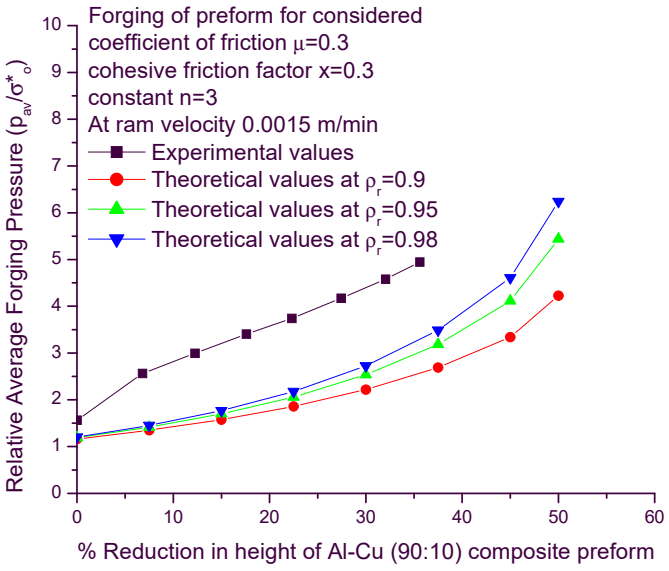

(c)

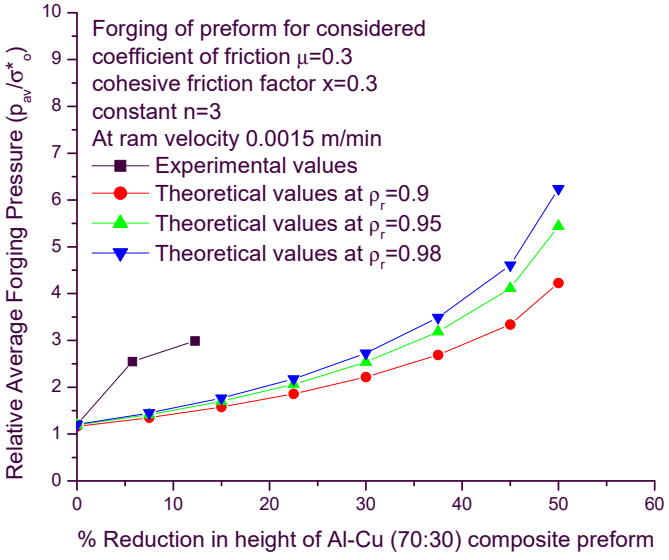

(d)

Figure 7 (a) Composite-preforms forged at ram velocity 1.5 mm/min (b) Composite-preforms forged at ram velocity 50 mm/min (c) Composite-preforms forged at ram velocity 100 mm/min (d) Composite-preforms forged at ram velocity 150 mm/min

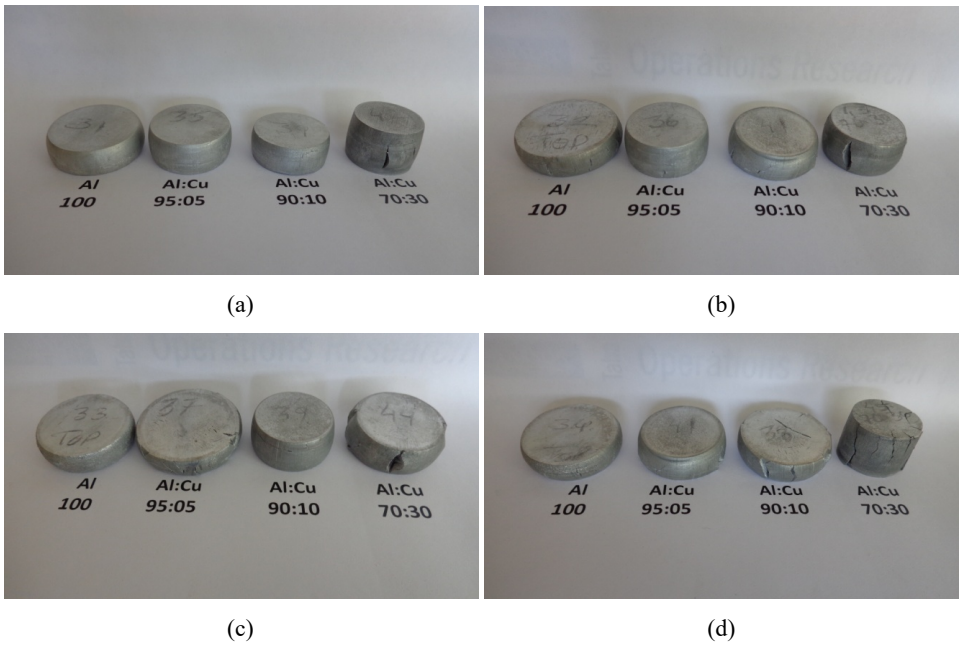

(a) (b)

(c) (d)

4 Results and discussions

The developed theory for the relative average forging pressure on the platen during forging of the composite preform at different strain rates (based on ram velocity) did not take in to account the changing relative density of the compressed preform. The parametric analysis had been done for the variation of one of the parameter keeping other parameters as constant. The experimental results coincide well with the theoretical results in the initial stage of the forging. This is quite evident from the results shown in Figures 6(a), 6(b), 6(c) and 6(d) for the relative average forging pressure versus percent reduction in height during forging at a considered ram velocity for the different compositions of the composite preforms. As the copper percentage was increasing in the composite preform, the deformation behaviour was changing from ductile to brittle. In fact this is a matter of critical study in powder metallurgy to ascertain at what composition and sintering temperature the deformation behaviour change from ductile to brittle of these composite preforms.

During the forging of the composite preforms, as the ram velocities were increased which resulted in increased relative average forging pressure (due to inertia effect), and percent reduction in height. This also resulted in appearance of crack on the equatorial free surfaces at lower percent reduction in height. The increased copper proportion in the composite preform was also one of the prominent factors for appearance of crack at lower percent reduction in height. Figures 7(a), 7(b), 7(c) and 7(d) show aluminium-copper composite preforms forged at ram velocities: 1.5, 50, 100 and 150 mm/min. The

forgeability of these preforms had been considered at the percent reduction in height at which cracks were observed by the naked eyes.

Figure 8 (a) Percent height reduction versus ram velocity (b) Forging stress versus ram velocity (c) Compressive strength versus ram velocity (d) Percent increase in bulge diameter versus ram velocity (e) Linear hoop strains versus ram velocity (see online version for colours)

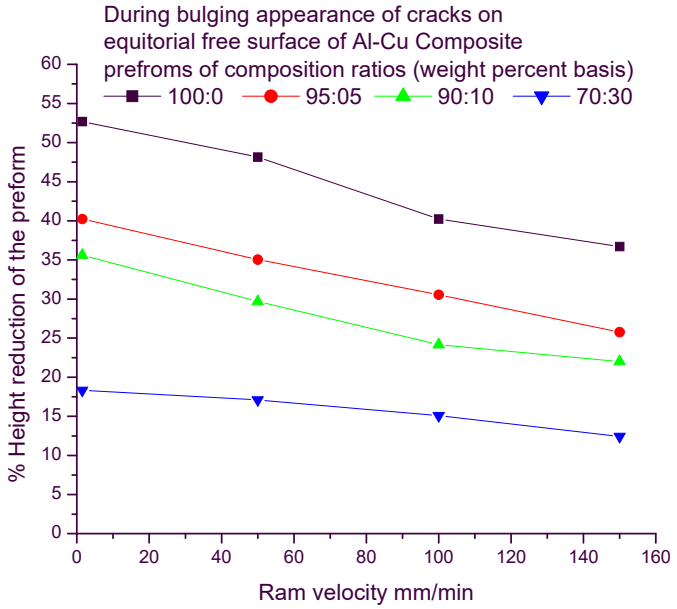

(a)

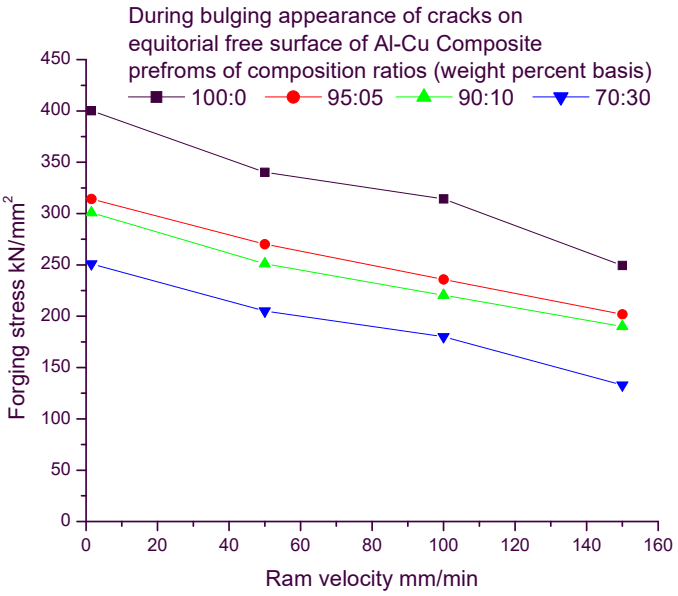

(b)

Figure 8 (a) Percent height reduction versus ram velocity (b) Forging stress versus ram velocity (c) Compressive strength versus ram velocity (d) Percent increase in bulge diameter versus ram velocity (e) Linear hoop strains versus ram velocity (continued) (see online version for colours)

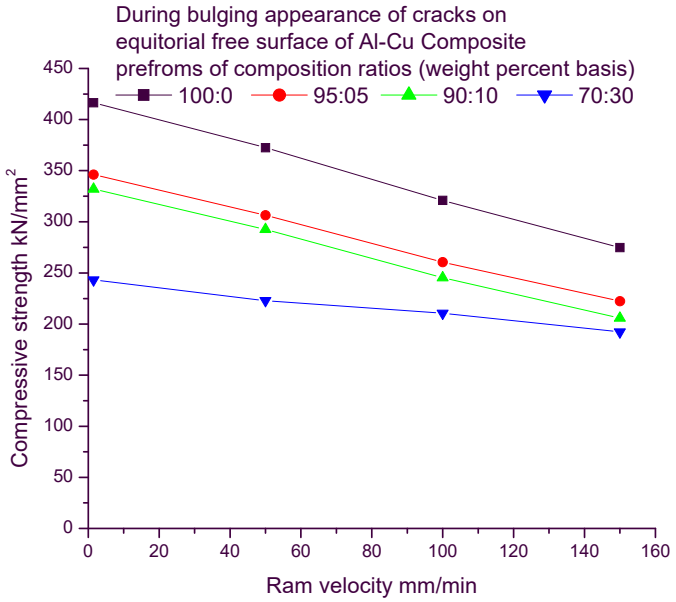

(c)

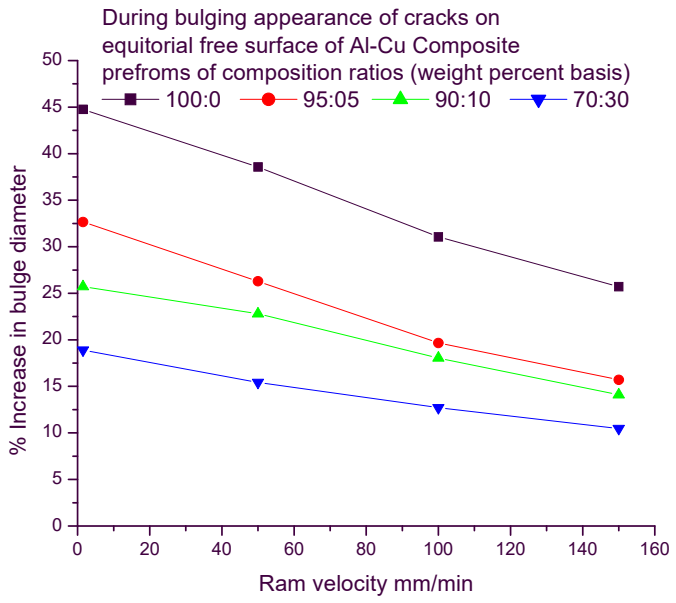

(d)

Figure 8 (a) Percent height reduction versus ram velocity (b) Forging stress versus ram velocity (c) Compressive strength versus ram velocity (d) Percent increase in bulge diameter versus ram velocity (e) Linear hoop strains versus ram velocity (continued) (see online version for colours)

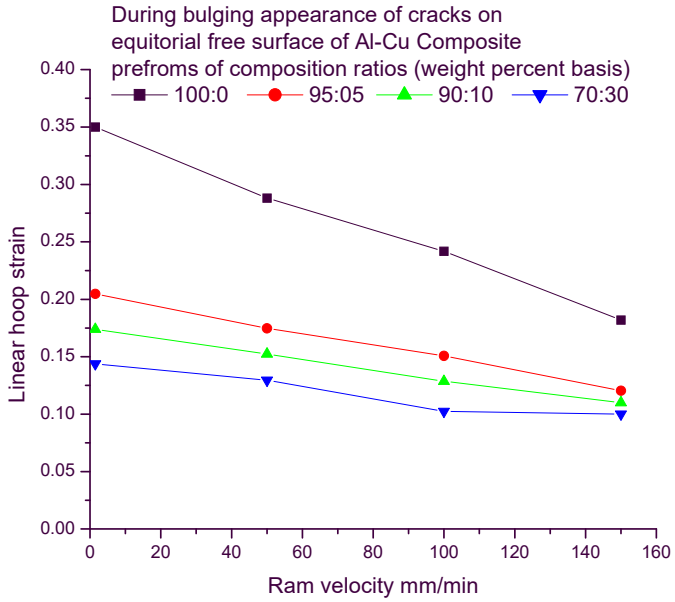

(e)

The deformation characteristics of the aluminium-copper composites preforms forged at ram velocities of 1.5, 50, 100 and 150 mm/min are shown in Figures 8(a), 8(b), 8(c), 8(d) and 8(e). Figure 8(a) shows the percent reduction in height of the preforms at which the cracks were observed by naked eyes versus ram velocity. For the ram velocities of 1.5, 50, 100 and 150 mm/min, the forgeability (percent reduction in height) of the preforms were observed as for: aluminium preforms at 52, 48, 42, and 38 respectively, aluminium-copper (95:05) composite preforms at 41, 36, 32, and 27% respectively, aluminium-copper (90:10) composite preforms at 36, 30, 25, and 23% respectively, and aluminium-copper (70:30) composite preforms at 18, 17, 15, and 13% respectively. The forgeability was falling with the increase of ram velocity as well as the percent increase in copper proportions in the composite. Figures 8(a), 8(b), 8(c), 8(d) and 8(e) show the other deformation characteristics of these composites in terms of the variation of: forging stress, compressive strength, percent increase in bulge diameters and linear hoop strain respectively versus ram velocity. All these deformation characteristics were decreasing with the increase of ram velocity.

References

Chitkara, N.R. and Bhutta, M.A. (2001) 'Dynamic heading of triangular, hexagonal, and octagonal shaped heads at high impact velocities: some experiments and an analysis', *International Journal Advanced Manufacturing Technology*, Vol. 18, pp.332–347, Springer-Verlag London Limited.

Cull, G.W. (1970) 'Mechanical and metallurgical properties of powder forging', *Powder Metallurgy*, Vol. 13, No. 26, p.156.

Deryagin, B.V. (1952) *What is Friction?*, Izd. Akad. Nauk USSR Moscow.

Jha, A.K. and Kumar, S. (1988) 'Deformation characteristics and fracture mechanism during the cold forging of metal powder preform', *Int. J. Mech. Tool Des. Res.*, Vol. 26, No. 4, p.369.

Ranjan, R.K. and Kumar, S. (2004a) 'An upper bound solution for closed die sinter forging of hexagonal shapes', *Sādhanā*, June, Vol. 29, Part 3, pp.263–273, ©Printed in India.

Ranjan, R.K. and Kumar, S. (2004b) 'High speed forging of solid powder polygonal discs with bulging', *Tamkang Journal of Science and Engineering*, Vol. 7, No. 4, pp.219–226.

Rooks, B.W. (1974) 'The effect of die temperature on metal flow and die wear during high speed hot forging', *15 The Int MTDR Conf.*, p.487.

Singh, S. and Jha, A.K. (2001) 'Analysis of dynamic effects during high sped forging of sintered preforms', *Journal of Materials Processing Technology*, Vol. 112, p.53, Elsevier.

Sumathi, M. and Selvakumar, N. (2012) 'An investigation on the workability of sintered copper-silicon carbide preforms during cold axial upsetting', *Indian Journal of Engineering & Materials Sciences*, April, Vol. 19, pp.121–128.

Tabata, T. and Masaki, M. (1978) 'A yield criterion for porous metals and analysis of axial compression of porous discs. Memories of Osaka Institute of Technology, Series-B', *Science and Technology*, Vol. 22, No. 2, p.45.

Verma, D., Chandrasekhar, P., Singh, S. and Kar, S. (2013) 'Investigations into deformation characteristics during open-die forging of SiCp reinforced aluminium metal matrix composites', *Journal of Powder Technology*, 14pp, Article ID 183713, Research Article, Hindawi Publishing Corporation.

Notations

ρ_r	relative density of the preform
ϕ_0	specific cohesion of the contact surface
λ	flow stress of the metal powder preform
k	constant equal to 2
η	function of relative density of preform
$d\lambda$	a positive constant
P	die-load
p	pressure
τ	shear stress
n	a constant quantity much greater than unity
μ	coefficient of friction
$\sigma_1, \sigma_2, \sigma_3$	principal stresses
$d\varepsilon_1, d\varepsilon_2, d\varepsilon_3$	principal-strain increments
x, y, z	Cartesian coordinates
r, θ, z	Polar coordinates
a	initial height of the preform

h	instantaneous thickness of the compressed preform
σ_0	yield stress of the non-work-hardening composite metal
σ_m	hydrostatic stress
J_2'	second invariant of the deviatoric stress
r_m	radius of the sticking zone

Subscripts

1 Initial condition

2 Final condition